The C-terminal Cytosolic Region of Rim21 Senses Alterations in Plasma Membrane Lipid Composition: Insights into Sensing Mechanisms for Plasma Membrane Lipid Asymmetry

Kanako Nishino*, Keisuke Obara*, and Akio Kihara

Faculty of Pharmaceutical Sciences, Hokkaido University, Sapporo, Japan
*These authors contributed equally to this work.

Running title: *Sensing mechanism by Rim21 C-terminal cytosolic region*

To whom correspondence should be addressed: Akio Kihara, Faculty of Pharmaceutical Sciences, Hokkaido University, Kita 12-jo Nishi 6-chome, Kita-ku, Sapporo 060-0812, Japan, Tel.: +81-11-706-3754; Fax: +81-11-706-4900; E-mail: kihara@pharm.hokudai.ac.jp

Key words: lipid bilayer, plasma membrane, yeast, phospholipid, signal transduction, lipid asymmetry, alkaline response, Rim21

Background: Sensing mechanism of lipid asymmetry and ambient-pH by Rim21 is unknown.
Results: The cytosolic region of Rim21 responded to alterations in the plasma membrane lipid composition and to external alkalization.
Conclusion: The cytosolic region of Rim21 acts as the sensor region.
Significance: Elucidating the sensing mechanism of Rim21 is important for understanding the maintenance of cell homeostasis of fungi.

ABSTRACT

Yeast responds to alterations in plasma membrane lipid asymmetry and external alkalization *via* the sensor protein Rim21 in the Rim101 pathway. However, the sensing mechanism used by Rim21 remains unclear. Here, we found that the C-terminal cytosolic domain of Rim21 (Rim21C) fused with GFP was associated with the plasma membrane under normal conditions, but dissociated upon alterations in lipid asymmetry or external alkalization. This indicates that Rim21C contains a sensor motif. Rim21C contains multiple clusters of charged residues. Among them, three consecutive Glu residues (EEE motif) were essential for Rim21 function and dissociation of Rim21C from the plasma membrane in response to changes in lipid asymmetry. In contrast, positively charged residues adjacent to the EEE motif were required for Rim21C to associate with the membrane. We therefore propose an "antenna hypothesis", in which Rim21C moves to or from the plasma membrane and functions as the sensing mechanism of Rim21.

In the plasma membrane lipid bilayer, lipid molecules are distributed unevenly between the inner (cytoplasmic) and outer (extracellular) leaflets. Phosphatidylserine (PtdSer) and phosphatidylethanolamine are mostly confined to the inner leaflet, while

complex sphingolipids are enriched in the outer leaflet (1,2). This phenomenon is called lipid asymmetry and is a common feature of the plasma membrane of eukaryotic cells. Lipid asymmetry does not come about spontaneously but is generated and regulated by ATP-dependent inward (flip) and outward (flop) trans-bilayer movements of lipid molecules, which are catalyzed by flippases and floppases, respectively (3-7).

Regulation of lipid asymmetry plays a central role in a great variety of cellular events, such as generation of membrane potential, vesicular transport, polarized cell growth, cell migration, blood coagulation, and removal of apoptotic cells (8-14). Yeast cells have five flippases in the P4-ATPase family (Dnf1, Dnf2, Dnf3, Drs2, and Neo1). Cells in which the *NEO1* gene has been deleted are inviable (4), and simultaneous deletion of the other four flippase genes is also lethal (13). These results highlight the essential role of lipid asymmetry in cell viability. In humans, impairment of the capacity to properly regulate lipid asymmetry is implicated in several diseases, such as intrahepatic cholestasis, Stargardt macular dystrophy, and Scott syndrome (9,15-17).

In the yeast *Saccharomyces cerevisiae*, alterations in lipid asymmetry caused by defective flip and/or flop functioning in phospholipids lead to activation of the Rim101 pathway (18), a signal transduction pathway that was first identified as an alkaline-responsive pathway (19). In the Rim101 pathway, a plasma membrane protein, Rim21, acts as the sensor protein for both altered lipid asymmetry and external alkalization (20). However, how this single sensor can sense both altered lipid asymmetry and external alkalization remains an enigma. Upon activation of the Rim101 pathway, expression of Rsb1 and Opt2, which are involved in the flop/transport of sphingoid long-chain bases and phospholipids, respectively, is induced (18,21-23).

Rim21 transduces the signal to downstream proteins in the Rim101 pathway, such as an arrestin-related protein Rim8, ESCRT proteins, a Bro1 domain-containing protein Rim20, and a calpain-like protein Rim13, at the plasma membrane (24-28). Rim13 then causes proteolytic activation of the transcription factor Rim101.

Rim21 is thought to span the membrane seven times, exposing its N-terminus and C-terminus to the extracellular and cytosolic space, respectively (20) (Fig. 1A). Rim21 does not have any regions that exhibit sequence similarity with known domains. The C-terminal cytosolic region of Rim21 (Rim21C) is unique in that charged amino acid residues are highly enriched (Fig. 1A). In the present study, we demonstrate that Rim21C senses altered lipid asymmetry and external alkalization. In addition, we identify motifs important for this sensing function using a systematic mutational analysis. From these results, we proposed an "antenna hypothesis" for the sensing mechanism employed by Rim21.

Experimental procedures

Yeast Strains and Media– *Saccharomyces cerevisiae* strains used in this study are listed in Table 1. Yeast cells were grown at 30 °C to log phase in YPD (1% yeast extract, 2% bactopeptone, 2% D-glucose) or synthetic complete (SC) medium (2% D-glucose and 0.67% yeast nitrogen base without amino acids, and appropriate supplements). Alkaline treatment was performed by adding 1 M Tris-HCl (pH 8.0) to the culture medium at a final concentration of 100 mM.

Genetic Manipulation and Plasmid Construction– Gene disruption was performed by replacing the entire coding region of the gene with a marker gene. Integration of P_{ADH}-*GFP-RIM21C* to the yeast chromosome was performed as follows. The P_{ADH}-*yEGFP* sequence was amplified by PCR from pYM9 (29) such that the *Sac*I and *Eco*RI sites were at the 5′ and 3′ ends, respectively, and a guanine was inserted after the *yEGFP* coding sequence to adjust the coding frame. The *RIM21C* sequence was amplified using PCR such that the *Eco*RI and *Xho*I sites were at the 5′ and 3′ ends, respectively. After digestion of their 5′ and 3′ ends with the respective restriction enzymes, these fragments were cloned together into the *Sac*I-*Xho*I site of p416CYC1 (30), generating pOK553. The *Sac*I-*Kpn*I fragment of pOK553 was excised and cloned into the *Sac*I-*Kpn*I site of pRS306 and pRS304 (31), creating pOK577 and pOK599, respectively. Introduction of point mutations was performed using the QuikChange site-directed mutagenesis kit (Agilent Technologies, Santa Clara, CA). We then linearized pOK577 and pOK599 *via* digestion by *Stu*I and *Hin*dIII, respectively, and inserted them into the *URA3* and *TRP1* loci, respectively.

Chromosomal fusion of the AID tag to the C-terminus of Neo1 was performed using PCR-based gene disruption and modification (32). The *FLAG-AID*, the *ADH1* terminator, and a marker sequence were amplified by PCR from the pFA6a vector series (32) with a primer set specific to *NEO1*. The amplified fragment was inserted into the chromosome by means of homologous recombination.

We constructed a *RIM21-C3-2×GFP* strain as follows. The *RIM21-2×GFP* sequence, including the *RIM21* promoter and *ADH* termination, was amplified using PCR from the genomic DNA of YOK3208 (*RIM21-2×GFP*) (20). The *Xho*I sites were at both the 5′ and the 3′ ends and the PCR product was cloned into the *Xho*I site of pRS306, generating pOK692. The C3 mutation was introduced into pOK692 using the QuickChange site-directed mutagenesis kit, creating pOK693. We then linearized pOK693 via digestion by *Stu*I and inserted it into the *URA3* locus of YOK2027 (*rim21*Δ) (20). Successful construction of the plasmids was confirmed by sequencing. Successful deletion of the genes and tagging were confirmed by genomic PCR, immunoblot analysis and/or fluorescence microscopy. The plasmid for the expression of HA-Rim101 (pFI1) was given to us by Dr. T. Maeda (The University of Tokyo, Japan).

Co-immunoprecipitation– Cells were cultured in YPD medium to log phase, harvested, suspended in lysis buffer [50 mM HEPES-NaOH (pH 8.0), 150 mM NaCl, 5 mM $MgCl_2$, 1 mM dithiothreitol, 1 mM PMSF, and EDTA-free protease inhibitor cocktail (Complete; Roche Diagnostics, Indianapolis, IN)], and broken by mixing vigorously with glass beads at 4 °C for 10 min. The cell lysates were sonicated and centrifuged at 5,000 × *g* for 3 min to remove cell debris. After treatment with 1% Triton X-100 at 4 °C for 1 h, samples were centrifuged at 100,000 × *g* for 30 min. The supernatant was then incubated with anti-FLAG M2 agarose beads (Sigma, St. Louis, MO) while rotating, and maintained at 4 °C for 90 min. The beads were washed three times with lysis buffer containing 0.1% Triton X-100. The bound proteins were eluted with SDS sample buffer and subjected to immunoblot analysis.

Immunoblot Analysis– Proteins were separated by SDS-PAGE and transferred to an Immobilon™ polyvinylidene difluoride

membrane (Millipore, Billerica, MA), as described previously (33). The membrane was incubated with anti-HA (TANA2; Medical & Biological Laboratories, Nagoya, Japan), anti-FLAG (M2; Stratagene), or anti-Pgk1 (Life Technologies, Carlsbad, CA) antibody. Signal detection was performed using Western Lightning ECL Pro system (PerkinElmer Life Sciences) with a bioimaging analyzer (LAS4000; Fuji Photo Film) or X-ray film. To detect Rim21-HA, proteins were deglycosylated as follows. The prepared total cell lysates were diluted with four volumes of endoglycosidase H (Endo H) buffer (62.5 mM sodium citrate (pH 5.5) and 1.25 mM PMSF) and incubated with 20 units/μl Endo H (Endo H_f, New England Biolabs, Beverly, MA) at 37 °C for 1 h with occasional mixing by tapping. Samples were then treated with an appropriate volume of 4× SDS sample buffer at 37°C for 10 min.

Microscopic Observation– Cells were grown to mid-log phase (OD_{600} = 1.2–2.0) and subjected to microscopic observation before and after alkaline treatment. Fluorescence of GFP was visualized under a fluorescence microscope (DM5000B, Leica Microsystems, Wetzlar, Germany) equipped with a cooled CCD camera (DFC365FX, Leica Microsystems) controlled with LAS AF software (version 2.60, Leica Microsystems). The images were archived using Photoshop CS3 (Adobe; San Jose, CA). *RIM21-2×GFP* and *RIM21-C3-2×GFP* cells were observed under a fluorescence microscope (IX-81, Olympus, Tokyo, Japan) equipped with an electron-multiplying CCD camera (ImagEM, C9100-13, Hamamatsu Photonics, Hamamatsu, Japan), controlled with MetaMorph software (Molecular Devices, Sunnyvale, CA). In some cases, a linear adjustment was applied to enhance the image contrast using the level adjustment function of Photoshop.

Quantification of fluorescence– All images were taken with the same exposure time, gain, and excitation intensity. The fluorescence of GFP-Rim21C was quantified using ImageJ software (http://imagej.nih.gov/ij/) as follows. The bud neck and some of the cytosol in a mother cell were isolated, avoiding strong signals from aggregates, and the mean fluorescence intensity of these areas were measured. The ratio of the mean fluorescence intensity of the bud neck to that of the cytosol was calculated for each cell. Three independent experiments, with at least 30 cells in each, were conducted, and the average of these was calculated. Results were tested for statistical significance using Student's *t* test.

Results

Rim21C dissociates from the plasma membrane in response to altered lipid asymmetry– To gain insight into the molecular mechanism by which Rim21 senses alternations in lipid asymmetry, we first focused on the C-terminal cytosolic region of Rim21 (Rim21C), where charged amino acid residues are highly enriched (Fig. 1A). Green fluorescent protein (GFP) was fused to Rim21C (GFP-Rim21C), and its localization was monitored. Although Rim21C does not apparently contain transmembrane segments, GFP-Rim21C was primarily detected at the plasma membrane in WT cells (Fig. 1B). Interestingly, a strong signal was often detected at the bud neck, where lipid asymmetry is known to be altered locally, *e.g.* where phosphatidylethanolamine is exposed to the outer leaflet (34). Some of the GFP-Rim21C was dispersed in the cytosol and the nucleus. Localization of GFP-Rim21C in the nucleus

may be the result of GFP's tendency to enter the nucleus.

Because Lem3 is a regulatory subunit of the flippases Dnf1 and Dnf2, plasma membrane lipid asymmetry is altered in *lem3*Δ cells as a result of inactivation of Dnf1 and Dnf2 (35,36). In *lem3*Δ cells, GFP-Rim21C completely dissociated from the plasma membrane and dispersed in the cytoplasm (Fig. 1B). A portion of GFP-Rim21C was detected as intense punctate signals, some of which were co-localized with Hsp104, a chaperone protein that refolds aggregated proteins, suggesting that excess GFP-Rim21C in the cytoplasm might sometimes form aggregates (Fig. 1C). Dissociation of GFP-Rim21 from the plasma membrane was also observed in deletion mutants for other flippase genes *DRS2* and *DNF3* (Fig. 1B).

For analysis of *NEO1*, which encodes another flippase essential for viability, we employed the auxin-inducible degron (AID) system in which proteins tagged with the AID tag can be degraded by the addition of a phytohormone auxin (37). We found that tagging Neo1 with the FLAG-AID tag itself caused a reduction in Neo1 function, as was evident from the observation that the *NEO1-FLAG-AID* strain was hypersensitive to neomycin (Fig. 1D). In this strain, GFP-Rim21C dissociated from the plasma membrane even without auxin treatment (Fig. 1B).

Lipid asymmetry is the result not only of flippases, but also of floppases. As for flippase gene disruption, deletion of the floppase *PDR5* gene caused dissociation of GFP-Rim21C from the plasma membrane (Fig. 1B). These observations indicate that Rim21C alone senses the status of lipid asymmetry and responds to alterations in lipid asymmetry. We evaluated the extent of its membrane binding by quantifying the ratio of the fluorescence intensity of the bud neck to that of the cytosol of the mother cell (Fig. 1E). Again, GFP-Rim21C clearly dissociated from the plasma membrane in mutants deficient in phospholipid flip/flop, although the degree of dissociation varied. Because Rim21C does not contain any transmembrane segments, it must be associated with the cytosolic surface of the plasma membrane. It is therefore highly likely that Rim21C recognizes changes in the membrane surface state on the basis of altered lipid asymmetry. We speculated that Rim21C senses the lipid composition of the inner leaflet of the plasma membrane. Indeed, a considerable fraction of GFP-Rim21C dissociated from the plasma membrane when PtdSer (enriched in the inner leaflet) was eliminated by deleting the sole PtdSer synthase gene *CHO1* (Fig. 1B and E).

We next investigated the dynamics of GFP-Rim21C after external alkalization and re-acidification, because Rim21 also senses external alkalization in addition to altered lipid asymmetry (20). Upon external alkalization, GFP-Rim21C dissociated from the plasma membrane and dispersed in the cytoplasm and the nucleus (Fig. 2). However, it re-attached to the plasma membrane within 5 min of re-acidification (which was achieved by transferring the cells to the normal acidic medium, at approximately pH 4.5; Fig. 2). This indicates that Rim21C can also sense changes in external pH.

Our findings show that Rim21C contains regions that can detect altered lipid asymmetry and external alkalization. In other words, a sensor motif capable of detecting lipid asymmetry and external alkalization exists in Rim21C.

A cluster of Glu residues in Rim21C is essential

for the sensing function– To identify the regions of Rim21C that play an important role in sensing lipid asymmetry and external alkalization, we performed a systematic mutational analysis of full-length Rim21. We created a series of Ala-substituted mutants of charged amino acid residue clusters (C1–C18; Fig. 1A) in Rim21C. Each mutant was expressed in *rim21*Δ cells from a low-copy (*CEN*) plasmid, and activation of the Rim101 pathway was monitored by detecting the processed form of Rim101. Rim21 contains three consecutive Glu residues (C3; amino acid 353-355; the EEE motif). The C3 mutant did not activate the Rim101 pathway upon external alkalization, indicating that the EEE motif is essential for Rim21 function (Fig. 3A). On the other hand, most Rim21 mutants did activate the Rim101 pathway, although their level of activity varied. For example, the C17 mutant, in which 13 acidic residues near the C-terminus were mutated, exhibited weak activity. This might have been the result of the low expression level of this mutant protein (Fig. 3A). However, no mutant exhibited constitutive activation of the Rim101 pathway without external alkalization (Fig. 3B).

We previously reported that Rim21 is modified by phosphorylation and *N*-glycosylation (20). In an immunoblot analysis of deglycosylated lysates, Rim21 was detected as two bands, the faster and slower migrating bands representing the unphosphorylated and phosphorylated forms, respectively (20). Two phosphorylation sites (Ser 409 and Ser 515, arrowheads in Fig. 1A) within Rim21C have been identified by comprehensive analysis (38,39). Both C6 and C2 mutant proteins, especially from alkali-treated cells, were detected as sharp single bands (Fig. 3A). The Ser 409 residue is adjacent to the C6 region, so phosphorylation at Ser 409 might be affected by C6 mutation. It is possible that C2 is located near the phosphorylation site in three-dimensional conformation. However, it should be noted that processing of Rim101 in response to external alkalization was normal in C2 and C6 mutants. This indicates that the banding pattern of Rim21, which probably represents its phosphorylation status, does not correlate with its function.

The EEE motif is involved in sensing altered lipid asymmetry– As described above, the C3 EEE motif was found to be essential for the functioning of Rim21 (Fig. 3A). We next examined which elementary processes the C3 EEE motif is involved in. Rim21 forms a complex with Dfg16, another component of the Rim101 pathway (20). HA-tagged Rim21-C3 mutant was co-immunoprecipitated with FLAG-tagged Dfg16, using anti-FLAG antibody. The efficiency of the immunoprecipitation was similar to that of Rim21 WT (Fig. 4A), indicating that the EEE motif is not essential for binding to Dfg16. Rim21 localizes primarily to the plasma membrane and partly to internal membrane structures (20). The Rim21-C3 mutant also did so (Fig. 4B), indicating that the EEE motif is not required for localization of Rim21 to the plasma membrane. At a later stage in Rim101 signaling, Rim20 is recruited to the plasma membrane, where it forms a protein complex that cleaves Rim101 (24,26). The accumulation of Rim20 in the plasma membrane did not occur in *rim21*Δ cells expressing the Rim21-C3 mutant (Fig. 4C), indicating that the EEE motif is a prerequisite for Rim20 recruitment to the plasma membrane.

We next analyzed the dynamics of GFP-Rim21C-C3, the GFP-fused, C-terminal domain of the Rim21-C3 mutant.

GFP-Rim21C-C3 was attached to the plasma membrane in WT cells, particularly at the bud neck, as was done with GFP-Rim21C (Fig. 4D and E). Interestingly, a large proportion of the GFP-Rim21C-C3 was still attached to the plasma membrane in the lipid asymmetry mutant (*lem3*Δ) and in the PtdSer-deficient mutant (*cho1*Δ). These observations indicate that Rim21C-C3 does not sense altered lipid asymmetry effectively; in other words, the EEE motif is necessary for sensing lipid asymmetry.

Because Rim21C was able to sense external alkalization as well as altered lipid asymmetry, we examined the localization of GFP-Rim21C-C3 after external alkalization. When the pH of the medium was increased to 8.0 from approximately 4.5, most of the GFP-Rim21C-C3 dissociated from the plasma membrane, like the GFP-Rim21C did (Fig. 5). In case the sudden increase in ambient pH to 8.0 was too drastic a change to properly test this mechanism, we repeated the test with a smaller increase in external pH, to 6.8. At this pH we still saw dissociation of GFP-Rim21C from the plasma membrane; however, a substantial fraction of GFP-Rim21-C3 remained bound to the inner leaflet (Fig. 5). The EEE motif is therefore also at least partly involved in sensing external alkalization.

Opposing effects of the EEE motif and the adjacent ERKEE motif regulates sensing of lipid asymmetry by Rim21– There is a cluster of charged amino acid residues (ERKEE, C2) adjacent to the EEE motif (C3; Fig. 1A). We examined the potential involvement of this motif in sensing lipid asymmetry and its interaction with the EEE motif. We found that GFP-Rim21C-C2 dissociated from the plasma membrane even in WT cells, in contrast to GFP-Rim21C (Fig. 6A and C). This effect was opposite to that of the EEE (C3) mutation. GFP-Rim21-C3 remained attached to the plasma membrane even in the lipid asymmetry mutant (*lem3*Δ; Figs. 4D and 6B). Introduction of both C2 and C3 mutations into GFP-Rim21C caused detachment of the resulting GFP-Rim21C-C2/C3 mutant from the plasma membrane (Fig. 6B and C). This suggests that the ERKEE and EEE motifs function in an antagonistic manner with respect to sensing of lipid asymmetry. The EEE motif contains only negatively charged residues, while the ERKEE motif has two positively charged residues (RK). Considering that Rim21C mostly dissociated from the plasma membrane in *cho1*Δ cells in which PtdSer, a negatively charged lipid, is absent, we speculated that positively charged RK sequence is involved in the association of Rim21C to the plasma membrane. Consistent with this assumption, GFP-Rim21C in which the RK sequence was substituted with AA [GFP-Rim21C-C2(AA)] dissociated from the plasma membrane of WT cells in a similar manner to the GFP-Rim21C-C2 mutant (Fig. 6A and C). Likewise, AA substitution of the RK sequence in the GFP-Rim21-C3 mutant caused detachment of the resulting GFP-Rim21C-C2(AA)/C3 protein from the plasma membrane in *lem3*Δ cells (Fig. 6B and C). These results indicate that the RK sequence within the C2 ERKEE motif is required for association of Rim21C with the plasma membrane. As already noted, the C2 mutation did not affect the ability of Rim21 to activate the Rim101 pathway (Fig. 3A), indicating that this motif is not essential for activation of the Rim101 pathway (see Discussion).

Discussion

We have demonstrated that Rim21C contains a region that functions to sense lipid

asymmetry and external alkalization (Figs 1 and 2). However, at present, we cannot exclude the possibility that the remainder of Rim21, which includes the N-terminal and transmembrane regions, is also partly involved in sensing lipid asymmetry and external alkalization. Within Rim21C, the C3 EEE and the C2 ERKEE motifs are important for the sensor function of Rim21 (Figs. 4 and 6). The EEE motif and the ERKEE motif seem to behave in an antagonistic manner: EEE is required for dissociation of Rim21C from the plasma membrane, while ERKEE, seems to be involved in the association of Rim21C with the plasma membrane. We speculate that the EEE and ERKEE motifs constitute the sensor motif and that altered lipid asymmetry is sensed by the balance between their counteracting effects. Mutation in the C3 EEE motif removed the ability of Rim21 to activate the Rim101 pathway (Fig. 3A), suggesting that dissociation of Rim21C from the plasma membrane is required for signal transduction to the downstream proteins. One may expect that mutation in C2 ERKEE causes the opposite effect to C3 mutation on the Rim101 pathway, *i.e.* stimulation and/or constitutive activation of the pathway. However, the Rim101 pathway was not constitutively activated under normal conditions in cells expressing the Rim21-C2 mutant, and the degree of activation of the Rim101 pathway upon external alkalization was indistinguishable between the WT and C2 mutants (Fig. 3), suggesting that dissociation of Rim21C from the plasma membrane alone is insufficient for activation of the Rim101 pathway. Alterations in lipid asymmetry and external alkalization may also cause some changes in Rim21 or other proteins of the Rim101 pathway. During preparation of this manuscript, it was reported that the activation threshold of the Rim101 pathway is regulated by phosphorylation of Rim8, a downstream molecule of Rim21 (40). Therefore, it is important that future investigations look at the relationship between Rim8 phosphorylation and how Rim21C associates with and dissociates from the plasma membrane.

The most important unsolved issue is the molecular mechanism of lipid asymmetry sensing. Rim21C is predicted to be broadly disordered (unstructured; Fig. 7A), suggesting that Rim21C is highly flexible. Based on this and the fact that Rim21C dissociates from the plasma membrane in response to altered lipid asymmetry (Fig. 1B), we propose the following working hypothesis. Rim21 uses its flexible C-terminal cytosolic tail (Rim21C) like an insect antenna to monitor the status of lipid asymmetry (Fig. 7B). Rim21C may associate with and dissociate from the plasma membrane using charged amino acid residues, particularly the ERKEE and EEE motifs. In the ERKEE motif, the positively charged amino acid residues, RK, mainly contribute to the association of Rim21C with the plasma membrane (Fig. 6). PtdSer is likely to be the main lipid involved in the interaction between Rim21C and the plasma membrane because Rim21C mostly dissociated from the plasma membrane in *cho1*Δ cells, in which PtdSer is absent (Fig. 1B). However, some of the Rim21C was still detectable on the plasma membrane in *cho1*Δ cells, suggesting that PtdSer is not the sole factor determining the affinity of Rim21C to the plasma membrane. Under normal conditions, ERKEE-mediated association with the plasma membrane is dominant. Alterations in lipid asymmetry cause changes in lipid composition and local charge on the inner leaflet, which can affect the balance between the ERKEE-mediated association with and

EEE-mediated repulsion from the plasma membrane, leading to dissociation of Rim21C from the plasma membrane. After Rim21C dissociates from the plasma membrane, downstream proteins in the Rim101 pathway may be recruited to Rim21.

Rim21 senses external alkalization as well as altered lipid asymmetry. How a single sensor can sense separate stimuli remains an enigma. We previously reported that the Rim101 pathway is activated by plasma membrane depolarization induced by a proton ionophore (20). The membrane potential of the yeast plasma membrane is mainly the result of differences in proton concentrations inside (pH = ~7.4) and outside the cells (pH = ~4.5). External alkalization therefore leads to plasma membrane depolarization. Rim21 may not recognize changes in lipid asymmetry or external alkalization through membrane potential, since Rim21C, which lacks transmembrane segments, responded to such changes. Rather, we speculate that Rim21C may detect changes in the lipid composition of the inner leaflet of the plasma membrane, as discussed above. A proton electrochemical gradient across the plasma membrane is required for phospholipid flipping (41). It is thus possible that Rim21C senses external alkalization through changes in the condition of the inner leaflet of the plasma membrane caused by impaired flipping as a result of plasma membrane depolarization.

Our findings provide a clue to understanding the molecular mechanism by which lipid asymmetry is sensed. However, further research is needed to elucidate the exact recognition target of Rim21C. In addition, further detailed analyses are necessary to confirm the antenna hypothesis.

Acknowledgments

We thank Dr. T. Maeda (The University of Tokyo) for providing the *HA-RIM101* plasmid (pFI1). We also thank Drs. Y. Ohsumi and H. Yamamoto (Tokyo Institute of Technology) for assistance in the microscopic observation. The AID system was provided by the National Bio-Resource Project (NBRP) of the MEXT, Japan. This work was supported by a Grant-in-Aid for Scientific Research (C) (25440038) and Grant-in-Aid for Young Scientists (B) (23770135) to KO and a Grant-in-Aid for Challenging Exploratory Research (25650059) to AK from the Japan Society for the Promotion of Science (JSPS). This work was also supported by Dr. Yoshifumi Jigami Memorial Fund from the Society of Yeast Scientists, by Grant for Basic Science Research Projects from The Sumitomo Foundation, and by a grant from the Institute for Fermentation, Osaka to KO.

Conflict of interest

The authors declare that they have no conflicts of interest with the contents of this article.

Author contributions

KN and KO performed the experiments. KO designed the experiments. NK, KO, and AK analyzed the data. KO and AK wrote the manuscript.

References

1. Devaux, P. F. (1991) Static and dynamic lipid asymmetry in cell membranes. *Biochemistry* **30**, 1163-1173
2. Verkleij, A. J., and Post, J. A. (2000) Membrane phospholipid asymmetry and signal transduction. *J. Membr. Biol.* **178**, 1-10
3. Axelsen, K. B., and Palmgren, M. G. (1998) Evolution of substrate specificities in the P-type ATPase superfamily. *J. Mol. Evol.* **46**, 84-101
4. Hua, Z., Fatheddin, P., and Graham, T. R. (2002) An essential subfamily of Drs2p-related P-type ATPases is required for protein trafficking between Golgi complex and endosomal/vacuolar system. *Mol. Biol. Cell* **13**, 3162-3177
5. Ikeda, M., Kihara, A., and Igarashi, Y. (2006) Lipid asymmetry of the eukaryotic plasma membrane: functions and related enzymes. *Biol. Pharm. Bull.* **29**, 1542-1546
6. Pomorski, T., Lombardi, R., Riezman, H., Devaux, P. F., van Meer, G., and Holthuis, J. C. (2003) Drs2p-related P-type ATPases Dnf1p and Dnf2p are required for phospholipid translocation across the yeast plasma membrane and serve a role in endocytosis. *Mol. Biol. Cell* **14**, 1240-1254
7. Seigneuret, M., and Devaux, P. F. (1984) ATP-dependent asymmetric distribution of spin-labeled phospholipids in the erythrocyte membrane: relation to shape changes. *Proc. Natl. Acad. Sci. U.S.A.* **81**, 3751-3755

8. Gurtovenko, A. A., and Vattulainen, I. (2008) Membrane potential and electrostatics of phospholipid bilayers with asymmetric transmembrane distribution of anionic lipids. *J. Phys. Chem. B* **112**, 4629-4634
9. Toti, F., Satta, N., Fressinaud, E., Meyer, D., and Freyssinet, J. M. (1996) Scott syndrome, characterized by impaired transmembrane migration of procoagulant phosphatidylserine and hemorrhagic complications, is an inherited disorder. *Blood* **87**, 1409-1415
10. Fadok, V. A., Voelker, D. R., Campbell, P. A., Cohen, J. J., Bratton, D. L., and Henson, P. M. (1992) Exposure of phosphatidylserine on the surface of apoptotic lymphocytes triggers specific recognition and removal by macrophages. *J. Immunol.* **148**, 2207-2216
11. Emoto, K., and Umeda, M. (2000) An essential role for a membrane lipid in cytokinesis. Regulation of contractile ring disassembly by redistribution of phosphatidylethanolamine. *J. Cell Biol.* **149**, 1215-1224
12. Chen, C. Y., Ingram, M. F., Rosal, P. H., and Graham, T. R. (1999) Role for Drs2p, a P-type ATPase and potential aminophospholipid translocase, in yeast late Golgi function. *J. Cell Biol.* **147**, 1223-1236
13. Furuta, N., Fujimura-Kamada, K., Saito, K., Yamamoto, T., and Tanaka, K. (2007) Endocytic recycling in yeast is regulated by putative phospholipid translocases and the Ypt31p/32p-Rcy1p pathway. *Mol. Biol. Cell* **18**, 295-312
14. Saito, K., Fujimura-Kamada, K., Hanamatsu, H., Kato, U., Umeda, M., Kozminski, K. G., and Tanaka, K. (2007) Transbilayer phospholipid flipping regulates Cdc42p signaling during polarized cell growth via Rga GTPase-activating proteins. *Dev. Cell* **13**, 743-751
15. Bull, L. N., van Eijk, M. J., Pawlikowska, L., DeYoung, J. A., Juijn, J. A., Liao, M., Klomp, L. W., Lomri, N., Berger, R., Scharschmidt, B. F., Knisely, A. S., Houwen, R. H., and Freimer, N. B. (1998) A gene encoding a P-type ATPase mutated in two forms of hereditary cholestasis. *Nat. Genet.* **18**, 219-224
16. Allikmets, R., Singh, N., Sun, H., Shroyer, N. F., Hutchinson, A., Chidambaram, A., Gerrard, B., Baird, L., Stauffer, D., Peiffer, A., Rattner, A., Smallwood, P., Li, Y., Anderson, K. L., Lewis, R. A., Nathans, J., Leppert, M., Dean, M., and Lupski, J. R. (1997) A photoreceptor cell-specific ATP-binding transporter gene (ABCR) is mutated in recessive Stargardt macular dystrophy. *Nat. Genet.* **15**, 236-246
17. Suzuki, J., Umeda, M., Sims, P. J., and Nagata, S. (2010) Calcium-dependent phospholipid scrambling by TMEM16F. *Nature* **468**, 834-U135
18. Ikeda, M., Kihara, A., Denpoh, A., and Igarashi, Y. (2008) The Rim101 pathway is involved in Rsb1 expression induced by altered lipid asymmetry. *Mol. Biol. Cell* **19**, 1922-1931
19. Peñalva, M. A., and Arst, H. N., Jr. (2004) Recent advances in the characterization of ambient pH regulation of gene expression in filamentous fungi and yeasts. *Annu. Rev.*

Microbiol. **58**, 425-451

20. Obara, K., Yamamoto, H., and Kihara, A. (2012) Membrane protein Rim21 plays a central role in sensing ambient pH in *Saccharomyces cerevisiae*. *J. Biol. Chem.* **287**, 38473-38481
21. Kihara, A., and Igarashi, Y. (2002) Identification and characterization of a *Saccharomyces cerevisiae* gene, *RSB1*, involved in sphingoid long-chain base release. *J. Biol. Chem.* **277**, 30048-30054
22. Yamauchi, S., Obara, K., Uchibori, K., Kamimura, A., Azumi, K., and Kihara, A. (2015) Opt2 mediates the exposure of phospholipids during cellular adaptation to altered lipid asymmetry. *J. Cell Sci.* **128**, 61-69
23. Kihara, A., and Igarashi, Y. (2004) Cross talk between sphingolipids and glycerophospholipids in the establishment of plasma membrane asymmetry. *Mol. Biol. Cell* **15**, 4949-4959
24. Obara, K., and Kihara, A. (2014) Signaling events of the Rim101 pathway occur at the plasma membrane in a ubiquitination-dependent manner. *Mol. Cell. Biol.* **34**, 3525-3534
25. Xu, W., and Mitchell, A. P. (2001) Yeast PalA/AIP1/Alix homolog Rim20p associates with a PEST-like region and is required for its proteolytic cleavage. *J. Bacteriol.* **183**, 6917-6923
26. Galindo, A., Calcagno-Pizarelli, A. M., Arst, H. N., Jr., and Peñalva, M. A. (2012) An ordered pathway for the assembly of fungal ESCRT-containing ambient pH signalling complexes at the plasma membrane. *J. Cell. Sci.* **125**, 1784-1795
27. Xu, W., Smith, F. J., Jr., Subaran, R., and Mitchell, A. P. (2004) Multivesicular body-ESCRT components function in pH response regulation in *Saccharomyces cerevisiae* and *Candida albicans*. *Mol. Biol. Cell* **15**, 5528-5537
28. Gomez-Raja, J., and Davis, D. A. (2012) The beta-arrestin-like protein Rim8 is hyperphosphorylated and complexes with Rim21 and Rim101 to promote adaptation to neutral-alkaline pH. *Eukaryot. Cell* **11**, 683-693
29. Janke, C., Magiera, M. M., Rathfelder, N., Taxis, C., Reber, S., Maekawa, H., Moreno-Borchart, A., Doenges, G., Schwob, E., Schiebel, E., and Knop, M. (2004) A versatile toolbox for PCR-based tagging of yeast genes: new fluorescent proteins, more markers and promoter substitution cassettes. *Yeast* **21**, 947-962
30. Mumberg, D., Muller, R., and Funk, M. (1995) Yeast vectors for the controlled expression of heterologous proteins in different genetic backgrounds. *Gene* **156**, 119-122
31. Sikorski, R. S., and Hieter, P. (1989) A system of shuttle vectors and yeast host strains designed for efficient manipulation of DNA in *Saccharomyces cerevisiae*. *Genetics* **122**, 19-27
32. Longtine, M. S., McKenzie, A., 3rd, Demarini, D. J., Shah, N. G., Wach, A., Brachat, A., Philippsen, P., and Pringle, J. R. (1998) Additional modules for versatile and economical PCR-based gene deletion and modification in *Saccharomyces cerevisiae*. *Yeast* **14**, 953-961

33. Obara, K., Kojima, R., and Kihara, A. (2013) Effects on vesicular transport pathways at the late endosome in cells with limited very long-chain fatty acids. *J. Lipid Res.* **54**, 831-842
34. Iwamoto, K., Kobayashi, S., Fukuda, R., Umeda, M., Kobayashi, T., and Ohta, A. (2004) Local exposure of phosphatidylethanolamine on the yeast plasma membrane is implicated in cell polarity. *Genes Cells* **9**, 891-903
35. Kato, U., Emoto, K., Fredriksson, C., Nakamura, H., Ohta, A., Kobayashi, T., Murakami-Murofushi, K., and Umeda, M. (2002) A novel membrane protein, Ros3p, is required for phospholipid translocation across the plasma membrane in *Saccharomyces cerevisiae*. *J. Biol. Chem.* **277**, 37855-37862
36. Saito, K., Fujimura-Kamada, K., Furuta, N., Kato, U., Umeda, M., and Tanaka, K. (2004) Cdc50p, a protein required for polarized growth, associates with the Drs2p P-type ATPase implicated in phospholipid translocation in *Saccharomyces cerevisiae*. *Mol. Biol. Cell* **15**, 3418-3432
37. Nishimura, K., Fukagawa, T., Takisawa, H., Kakimoto, T., and Kanemaki, M. (2009) An auxin-based degron system for the rapid depletion of proteins in nonplant cells. *Nat. Methods* **6**, 917-922
38. Albuquerque, C. P., Smolka, M. B., Payne, S. H., Bafna, V., Eng, J., and Zhou, H. (2008) A multidimensional chromatography technology for in-depth phosphoproteome analysis. *Mol. Cell. Proteomics* **7**, 1389-1396
39. Bodenmiller, B., Campbell, D., Gerrits, B., Lam, H., Jovanovic, M., Picotti, P., Schlapbach, R., and Aebersold, R. (2008) PhosphoPep--a database of protein phosphorylation sites in model organisms. *Nat. Biotech.* **26**, 1339-1340
40. Herrador, A., Livas, D., Soletto, L., Becuwe, M., Léon, S., and Vincent, O. (2015) Casein kinase 1 controls the activation threshold of an alpha-arrestin by multisite phosphorylation of the interdomain hinge. *Mol. Biol. Cell* **26**, 2128-2138
41. Stevens, H. C., and Nichols, J. W. (2007) The proton electrochemical gradient across the plasma membrane of yeast is necessary for phospholipid flip. *J. Biol. Chem.* **282**, 17563-17567
42. Robinson, J. S., Klionsky, D. J., Banta, L. M., and Emr, S. D. (1988) Protein sorting in *Saccharomyces cerevisiae*: isolation of mutants defective in the delivery and processing of multiple vacuolar hydrolases. *Mol. Cell. Biol.* **8**, 4936-4948

Abbreviations used in this paper

Rim21C, C-terminal cytosolic domain of Rim21; PtdSer, phosphatidylserine; AID, auxin-inducible degron; SC, synthetic complete

Figure Legends

FIGURE 1. **Rim21C senses altered lipid asymmetry.** *A*, Predicted membrane topology of Rim21 and amino acid sequences of the C-terminal cytosolic region of Rim21 (Rim21C). Positively and negatively charged amino acid residues are depicted in blue and red, respectively. Clusters of charged amino acid residues C1-C18 are boxed. Arrowheads indicate phosphorylated amino acid residues. *B*, YOK3395 (*GFP-RIM21C*), YOK3396 (*GFP-RIM21C*, *lem3*Δ), YKN58 (*GFP-RIM21C*, *drs2*Δ), YOK3700 (*GFP-RIM21C*, *dnf3*Δ), YOK3397 (*GFP-RIM21C*, *pdr5*Δ), YOK3398 (*GFP-RIM21C*, *cho1*Δ), and YOK3689 (*GFP-RIM21C NEO1-FLAG-AID*) cells were grown to log phase in SC medium and photographed under a fluorescence microscope. Scale bar is 5 μm. *C*, YOK3441 (*GFP-RIM21C HSP104-RedStar2 lem3*Δ) cells were grown to log phase and photographed using a fluorescence microscope. Scale bar is 5 μm. *D*, YOK3073 (WT) and YOK3684 (*NEO1-FLAG-AID*) cells were grown to stationary phase, serially diluted at 1:10, spotted on YPD plates with or without 1 mg/mL neomycin, and grown at 30 °C for 24 h or 48 h, as indicated. *E*, Ratio of fluorescence of bud neck to cytosol for all seven strains in B. Values represent means ± SD of three independent experiments (* $P < 0.05$).

FIGURE 2. **Rim21C senses changes in ambient pH.** *A*, YOK3395 (*GFP-RIM21C*) cells were grown to log phase in SC medium and observed before and 20 min after treatment with an alkaline solution (pH 8.0; upper panels). After alkaline treatment, cells were kept in the same medium for another 20 min or transferred back to SC medium and incubated for 5 min (lower panels). Cells were then observed under a fluorescence microscope. Scale bar is 5 μm. *B*, Ratio of fluorescence of bud neck to cytosol at the different treatment stages. Values represent means ± SD of three independent experiments (* $P < 0.05$; ** $P < 0.01$).

FIGURE 3. **The EEE motif is essential for Rim21 functioning.** YOK2027 (*rim21*Δ) cells expressing HA-Rim101 and one of the Rim21 mutants were grown to log phase and collected before (B) and 20 min after (A) alkaline treatment (pH 8.0). Total lysates were prepared and analyzed by immunoblotting with anti-HA antibody. The experiments were repeated three times, with similar results. The asterisk indicates a non-specific band. FL and DC denote full-length and processed Rim101, respectively. The resultant Rim21 mutants were as follows: C1, DR to AA; C2, ERKEE to AAAAA; C3 EEE to AAA; C4, RRE to AAA; C5, DRHD to AAAA; C6, RYDPED to

AYAPAA; C7, RSIDR to ASIAA; C8, HFNDR to AFNAA; C9, KD to AA; C10, KK to AA; C11, RDK to AAA; C12, KNEKTK to ANAATA; C13, RK to AA; C14, RKR to AAA; C15, DK to AA; C16, KD to AA; C17, DEDDDENAEDEDDDE to AAAAAANAAAAAAAA; and C18, DHIGH to AAIGA.

FIGURE 4. **The EEE motif is involved in sensing altered lipid asymmetry.** *A*, Total lysates were prepared from YOK3764 (*RIM21-HA*), YOK3761 (*RIM21-HA DFG16-FLAG*), YKN152 (*RIM21-C3-HA*), and YOK3462 (*RIM21-C3-HA DFG16-FLAG*), solubilized with Triton X-100, and immunoprecipitated using anti-FLAG antibody conjugated to agarose beads. Immunoprecipitates were separated by SDS-PAGE and detected by immunoblotting with anti-HA and anti-FLAG antibodies. Asterisks indicate nonspecific bands. IP: immunoprecipitation. *B*, YOK3208 (*RIM21-GFP*) and YOK3842 (*RIM21-C3-GFP*) cells were grown to log phase in SC medium and photographed under a fluorescence microscope. Scale bar is 5 μm. *C*, YOK3249 (*RIM20-GFP rim21*Δ) cells harboring an empty vector (vec), pOK648 (*RIM21*), or pOK649 (*RIM21-C3*) were photographed under a fluorescence microscope after treatment with an alkaline solution for 60 min. Scale bar is 5 μm. *D*, YOK3395 (*GFP-RIM21C*), YOK3396 (*GFP-RIM21C lem3*Δ), YOK3398 (*GFP-RIM21C cho1*Δ), YOK3399 (*GFP-RIM21C-C3*), YOK3405 (*GFP-RIM21C-C3 lem3*Δ), and YOK3402 (*GFP-RIM21C-C3 cho1*Δ) were grown to log phase in SC medium and photographed under a fluorescence microscope. Scale bar is 5 μm. *E*, Ratio of fluorescence of bud neck to cytosol for the six strains in D. Values represent means ± SD of three independent experiments (* $P < 0.05$; ** $P < 0.01$).

FIGURE 5. **The EEE motif is involved in sensing external alkalization.** *A*, YOK3395 (*GFP-RIM21C*) and YOK3399 (*GFP-RIM21C-C3*) cells were grown to log phase and photographed under a fluorescence microscope before and 20 min after changing the ambient pH. Scale bar is 5 μm. *B*, Ratio of fluorescence of bud neck to cytosol for the two strains at the different treatment stages. Values represent means ± SD of three independent experiments (* $P < 0.05$; ** $P < 0.01$).

FIGURE 6. **The ERKEE motif counteracts the EEE motif in sensing changes in lipid asymmetry.** *A*, YOK3395 (*GFP-RIM21C*), YKN150 (*GFP-RIM21C-C2*), and YOK3791 [*GFP-RIM21C-C2(AA)*] cells were grown in SC medium to log phase and photographed under a fluorescence microscope. Scale bar is 5 μm. *B*, YOK3396 (*GEP-RIM21C lem3*Δ), YOK3405 (*GEP-RIM21C-C3 lem3*Δ), YOK3437 (*GEP-RIM21C-C2/C3 lem3*Δ), and YOK3797 [*GFP-RIM21C-C2(AA)/C3 lem3*Δ] cells were grown in SC medium to log phase and photographed under a fluorescence microscope. Scale bar is 5 μm. *B*, Ratio of fluorescence of bud neck to cytosol for all seven strains. Values represent means ± SD of three independent experiments (* $P < 0.05$; **

$P < 0.01$).

FIGURE 7. **Antenna hypothesis.** *A*, The disordered state of Rim21C, as predicted by DRIPPred program (http://www.sbc.su.se/~maccallr/disorder/). Disordered and ordered regions are shown in red and blue, respectively. The ERKEE and EEE motifs are boxed. *B*, Illustration of a working hypothesis concerning the mechanism by which lipid asymmetry is sensed. Rim21 uses its flexible C-terminal cytosolic region (Rim21C) like an insect antenna to monitor lipid asymmetry by sensing the state of the cytosolic surface of the plasma membrane. The ERKEE motif, especially the positively charged RK residues, mediates association of Rim21C with the plasma membrane, while the EEE motif promotes repulsion from the plasma membrane. Usually the ERKEE-mediated association is dominant. When lipid asymmetry is altered, changes occur in the balance between the effects of these two motifs. As a result, the EEE-mediated repulsion of Rim21C becomes dominant. Rim21C dissociates from the plasma membrane, is then recognized by downstream proteins in the Rim101 pathway and activates signal transduction.

TABLE 1. Yeast strains used in this study

Strain	Genotype	Source
SEY6210	*MATα his3 leu2 ura3 trp1 lys2 suc2*	(42)
YOK2027	SEY6210, *rim21Δ::KanMX4*	(20)
YOK2543	SEY6210, *pep4Δ::LEU2 prb1Δ::NatNT2 DFG16-FLAG::KanMX6*	This study
YOK3073	SEY6210, P_{ADH}*-OsTIR1-Myc::URA3*	(24)
YOK3208	SEY6210, *RIM21-2×GFP::KanMX6*	(20)
YOK3249	SEY6210, *RIM20-GFP::TRP1 rim21Δ::KanMX4*	This study
YOK3395	SEY6210, P_{ADH}*-GFP-RIM21C::URA3*	This study
YOK3396	SEY6210, P_{ADH}*-GFP-RIM21C::URA3 lem3Δ::KanMX4*	This study
YOK3397	SEY6210, P_{ADH}*-GFP-RIM21C::URA3 pdr5Δ::KanMX4*	This study
YOK3398	SEY6210, P_{ADH}*-GFP-RIM21C::URA3 cho1Δ::KanMX4 RSB1-HA::TRP1*	This study
YOK3399	SEY6210, P_{ADH}*-GFP-RIM21C(E353A E354A E355A)::URA3*	This study
YOK3402	SEY6210, P_{ADH}*-GFP-RIM21C(E353A E354A E355A)::URA3 cho1Δ::KanMX4 RSB1-HA::TRP1*	This study
YOK3405	SEY6210, P_{ADH}*-GFP-RIM21C(E353A E354A E355A)::URA3 lem3Δ::NatNT2*	This study
YOK3437	SEY6210, P_{ADH}*-GFP-RIM21C(E338A R339A K340A E341A E342A E353A E354A E355A)::URA3 lem3Δ::KanMX4*	This study
YOK3441	SEY6210, P_{ADH}*-GFP-RIM21C::URA3 HSP104-RedStar2::NatNT2 lem3Δ::KanMX4*	This study
YOK3684	SEY6210, P_{ADH}*-OsTIR1-Myc::URA3 NEO1-FLAG-AID::KanMX6*	This study
YOK3689	SEY6210, P_{ADH}*-OsTIR1-Myc::URA3 NEO1-FLAG-AID::KanMX6* P_{ADH}*-GFP-RIM21C::TRP1*	This study
YOK3700	SEY6210, P_{ADH}*-GFP-RIM21C::URA3 dnf3Δ::KanMX4*	This study
YOK3761	SEY6210, *pep4Δ::LEU2 prb1Δ::NatNT2 DFG16-FLAG::KanMX6 rim21Δ::TRP1 RIM21-HA::URA3*	This study
YOK3762	SEY6210, *pep4Δ::LEU2 prb1Δ::NatNT2 DFG16-FLAG::KanMX6 rim21Δ::TRP1 RIM21(E353A E354A E355A)-HA::URA3*	This study
YOK3764	SEY6210, *pep4Δ::LEU2 prb1Δ::NatNT2 rim21Δ::TRP1 RIM21-HA::URA3*	This study
YOK3791	SEY6210, P_{ADH}*-GFP-RIM21C(R339A K340A)::URA3*	This study
YOK3797	SEY6210, P_{ADH}*-GFP-RIM21C(R339A K340A E353A E354A E355A)::URA3 lem3Δ::KanMX4*	This study
YOK3842	SEY6210, *rim21Δ::KanMX4 RIM21-C3-2×GFP::URA3*	This study

YKN58	SEY6210, P_{ADH}-*GFP-RIM21C::URA3 drs2*Δ*::KanMX4*	This study
YKN150	SEY6210, P_{ADH}-*GFP-RIM21C(E338A R339A K340A E341A E342A)::URA3*	This study
YKN152	SEY6210, *pep4*Δ*::LEU2 prb1*Δ*::NatNT2 rim21*Δ*::TRP1 RIM21(E353A E354A E355A)-HA::URA3*	This study

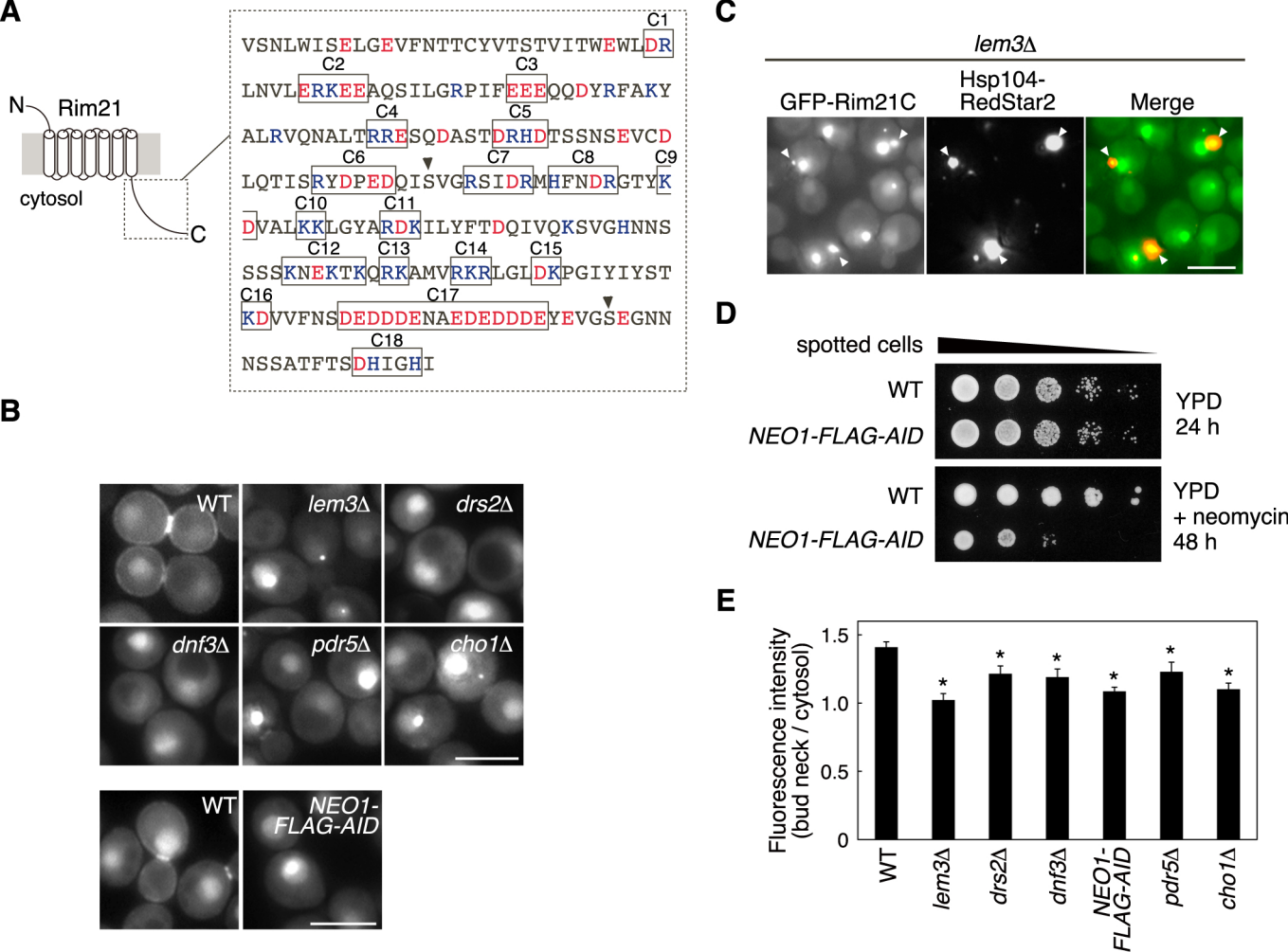
A
N
Rim21
cytosol
C
C1
VSNLWISELGEVFNTTCYVTSTVITWEWLDR
C2
C3
LNVLERKEEAQSILGRPIFEEEQQDYRFAKY
C4
C5
ALRVQNALTRRESQDASTDRHDTSSNSEVCD
C6
C7
C8
C9
LQTISRYDPEDQISVGRSIDRMHFNDRGTYK
C10
C11
DVALKKLGYARDKILYFTDQIVQKSVGHNNS
C12
C13
C14
C15
SSSKNEKTKQRKAMVRKRLGLDKPGIYIYST
C16
C17
KDVVFNSDEDDDENAEDEDDDEYEVGSEGNN
C18
NSSATFTSDHIGHI
B
WT
lem3Δ
drs2Δ
dnf3Δ
pdr5Δ
cho1Δ
WT
NEO1-FLAG-AID
C
lem3Δ
GFP-Rim21C
Hsp104-RedStar2
Merge
D
spotted cells
WT
NEO1-FLAG-AID
YPD
24 h
WT
NEO1-FLAG-AID
YPD
+ neomycin
48 h
E
Fluorescence intensity (bud neck / cytosol)
1.5
1.0
0.5
0
WT
lem3Δ
drs2Δ
dnf3Δ
NEO1-FLAG-AID
pdr5Δ
cho1Δ

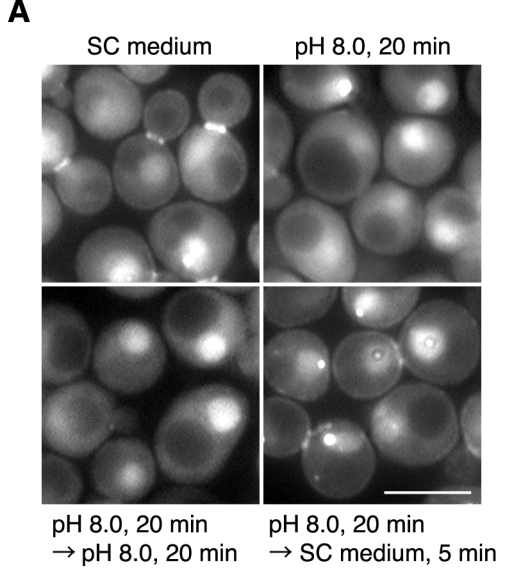
A
SC medium
pH 8.0, 20 min
pH 8.0, 20 min
→ pH 8.0, 20 min
pH 8.0, 20 min
→ SC medium, 5 min

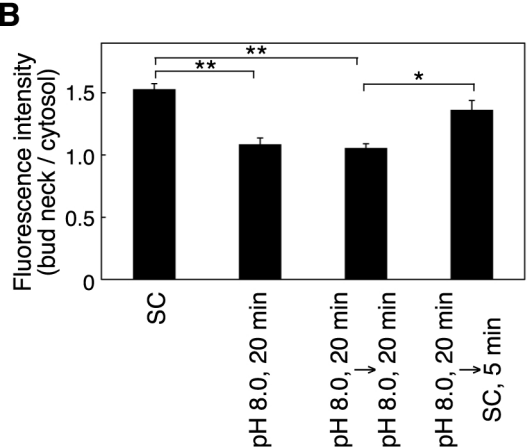
B
Fluorescence intensity
(bud neck / cytosol)
0
0.5
1.0
1.5
**
**
*
SC
pH 8.0, 20 min
pH 8.0, 20 min
→
pH 8.0, 20 min
pH 8.0, 20 min
→
SC, 5 min

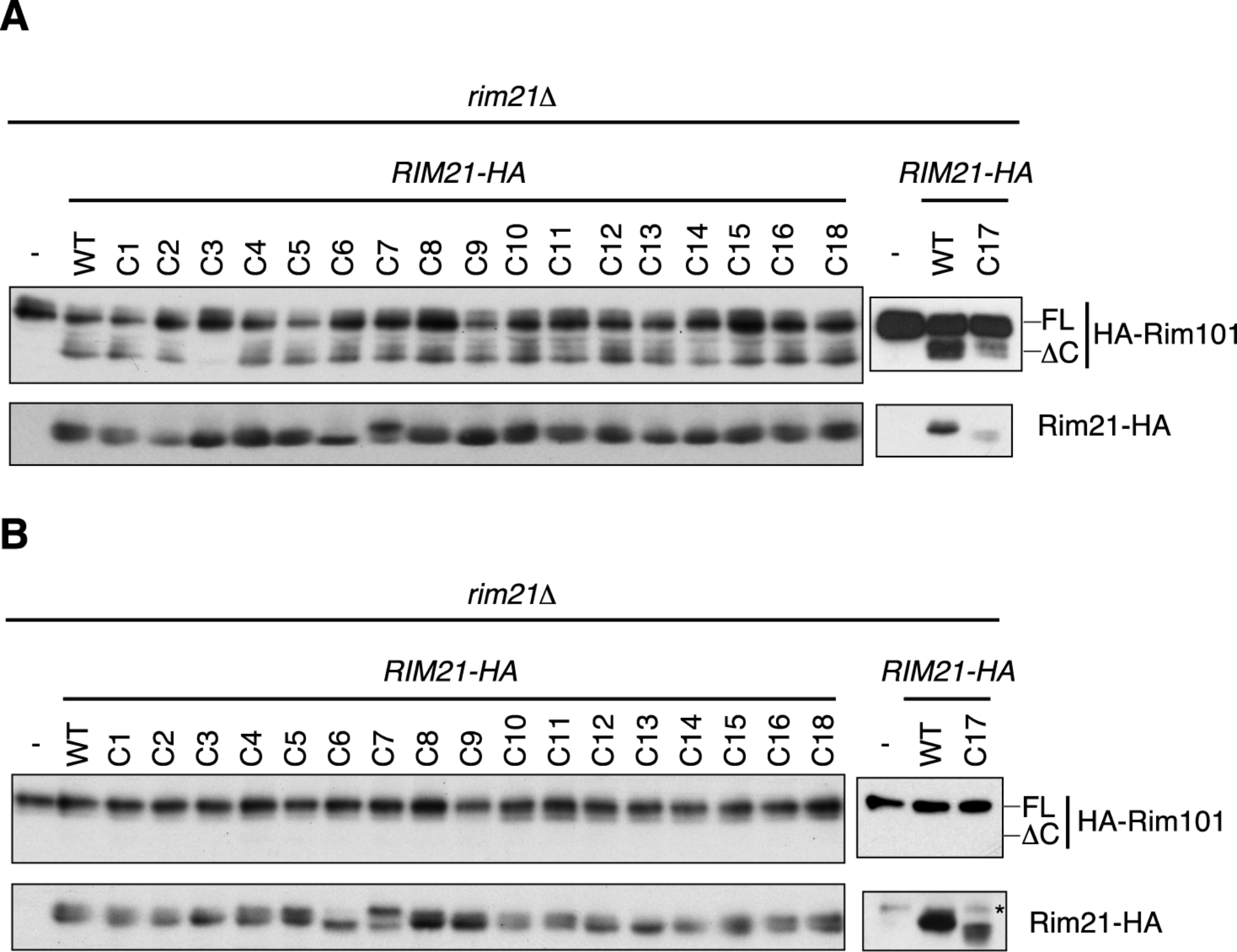
A
rim21Δ
RIM21-HA
RIM21-HA
-
WT
C1
C2
C3
C4
C5
C6
C7
C8
C9
C10
C11
C12
C13
C14
C15
C16
C18
-
WT
C17
FL
ΔC
HA-Rim101
Rim21-HA
B
rim21Δ
RIM21-HA
RIM21-HA
-
WT
C1
C2
C3
C4
C5
C6
C7
C8
C9
C10
C11
C12
C13
C14
C15
C16
C18
-
WT
C17
FL
ΔC
HA-Rim101
*
Rim21-HA

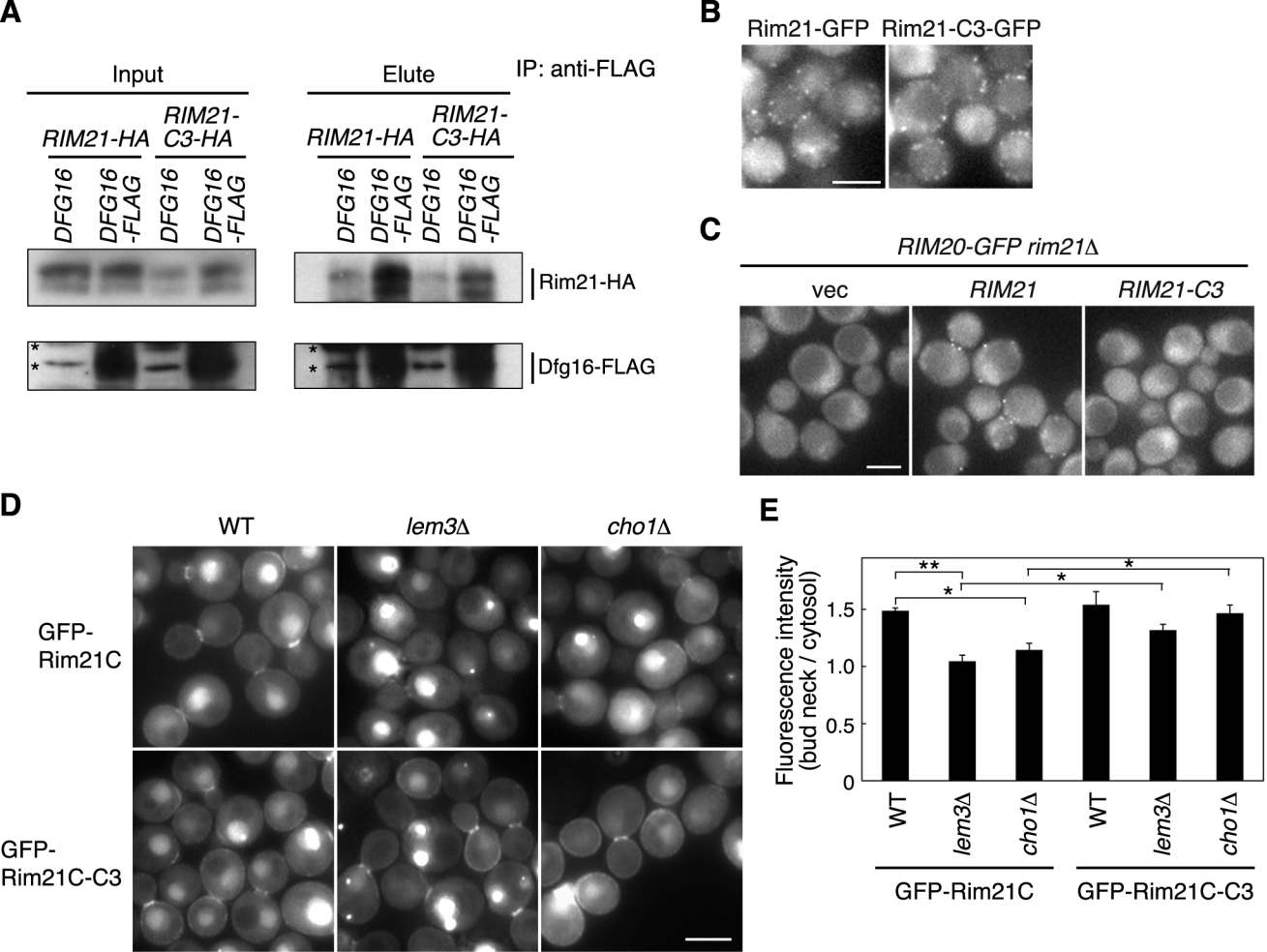
A
Input
Elute
IP: anti-FLAG
RIM21-HA
RIM21-C3-HA
DFG16
DFG16-FLAG
Rim21-HA
Dfg16-FLAG
B
Rim21-GFP
Rim21-C3-GFP
C
RIM20-GFP rim21Δ
vec
RIM21
RIM21-C3
D
WT
lem3Δ
cho1Δ
GFP-Rim21C
GFP-Rim21C-C3
E
Fluorescence intensity (bud neck / cytosol)
0
0.5
1
1.5
**
*
*
*
WT
lem3Δ
cho1Δ
WT
lem3Δ
cho1Δ
GFP-Rim21C
GFP-Rim21C-C3

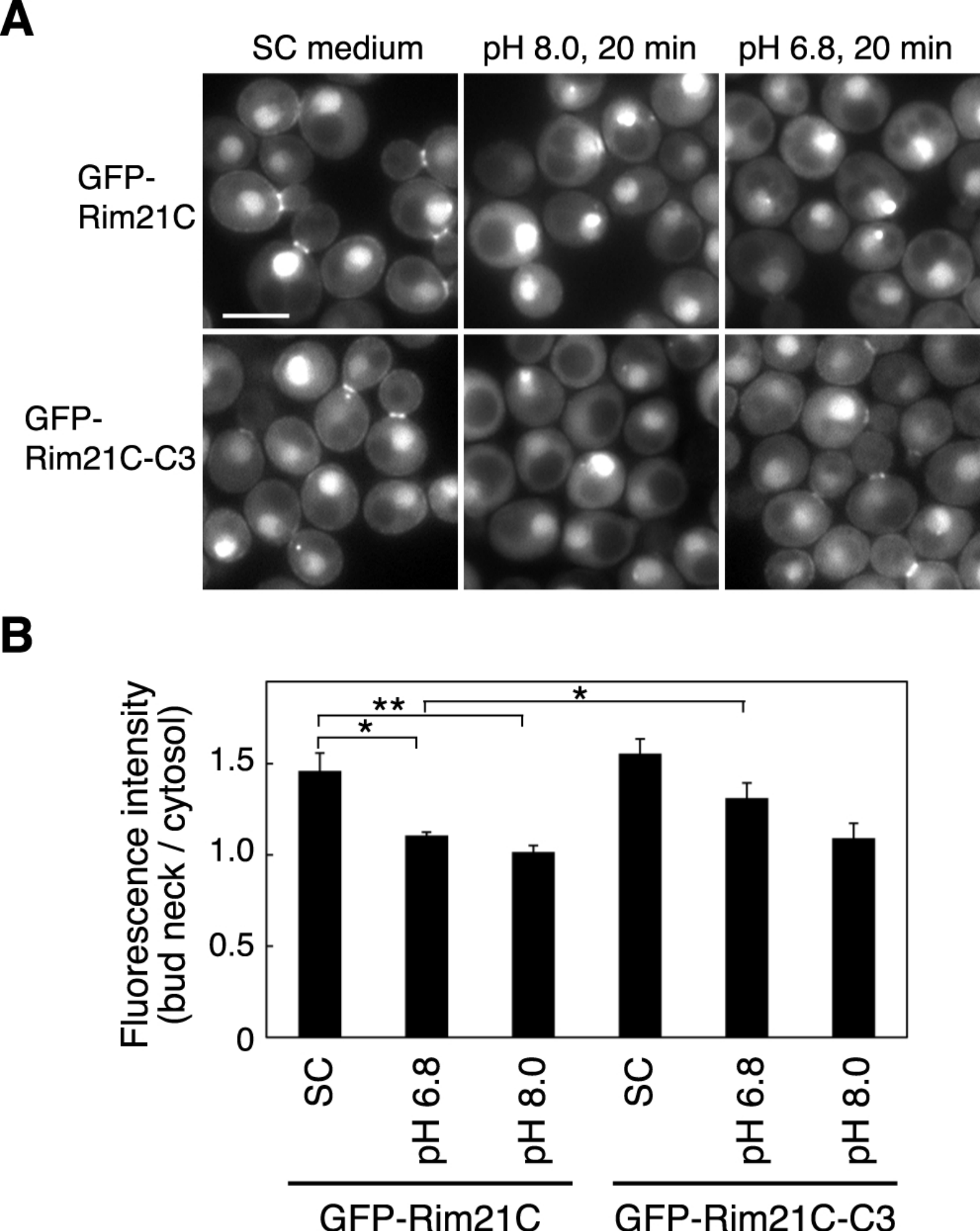
A
SC medium
pH 8.0, 20 min
pH 6.8, 20 min
GFP-Rim21C
GFP-Rim21C-C3
B
Fluorescence intensity (bud neck / cytosol)
0
0.5
1.0
1.5
**
*
*
SC
pH 6.8
pH 8.0
SC
pH 6.8
pH 8.0
GFP-Rim21C
GFP-Rim21C-C3

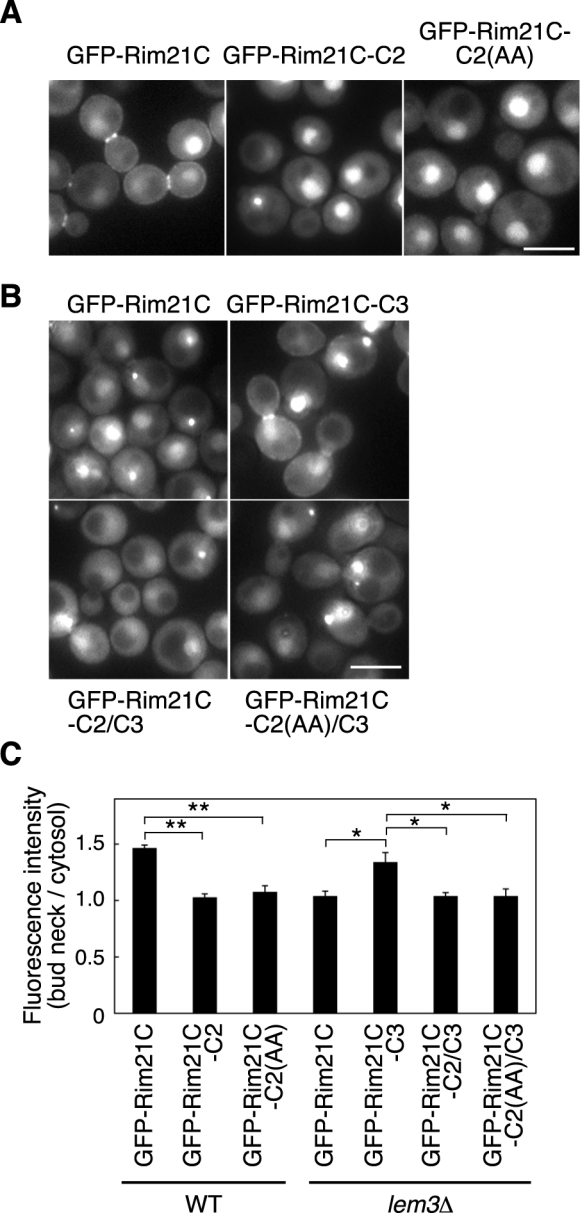
A
GFP-Rim21C
GFP-Rim21C-C2
GFP-Rim21C-C2(AA)
B
GFP-Rim21C
GFP-Rim21C-C3
GFP-Rim21C-C2/C3
GFP-Rim21C-C2(AA)/C3
C
Fluorescence intensity (bud neck / cytosol)
0
0.5
1
1.5
**
**
*
*
*
GFP-Rim21C
GFP-Rim21C-C2
GFP-Rim21C-C2(AA)
GFP-Rim21C
GFP-Rim21C-C3
GFP-Rim21C-C2/C3
GFP-Rim21C-C2(AA)/C3
WT
lem3Δ

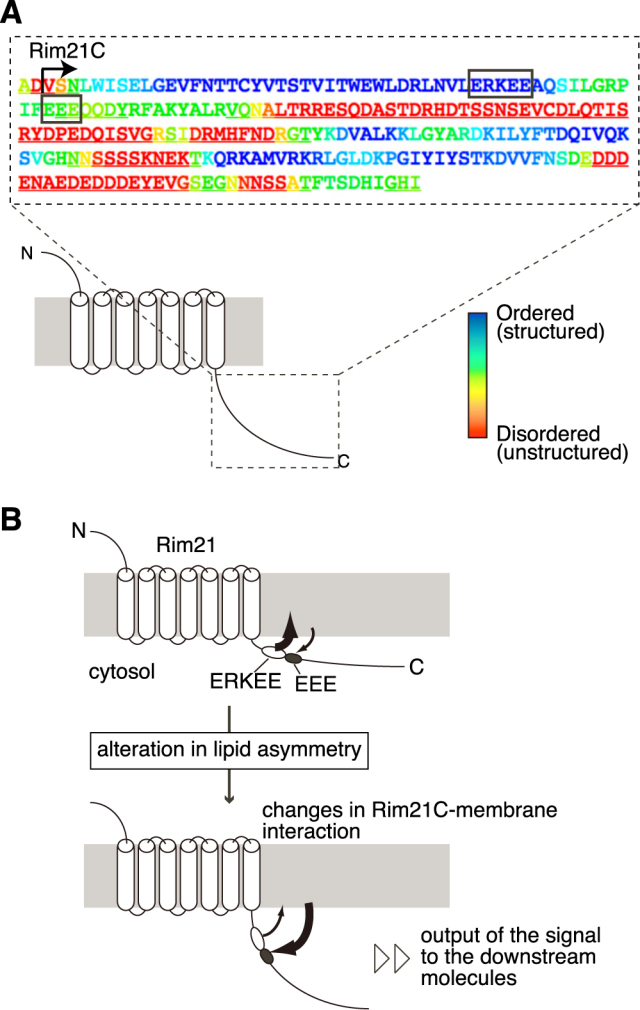
A
Rim21C
ADVSNLWISELGEVFNTTCYVTSTVITWEWLDRLNVLERKEEAQSILGRP
IFEEEDQDYRFAKYALRVQNALTRRESQDASTDRHDTSSNSEVCDLQTIS
RYDPEDQISVGRSIDRMHFNDRGTYKDVALKKLGYARDKILYFTDQIVQK
SVGHNNSSSSKNEKTKQRKAMVRKRLGLDKPGIYIYSTKDVVFNSDEDDD
ENAEDEDDDEYEVGSEGNNNSSATFTSDHIGHI
N
C
Ordered
(structured)
Disordered
(unstructured)
B
N
Rim21
cytosol
ERKEE
EEE
C
alteration in lipid asymmetry
changes in Rim21C-membrane
interaction
output of the signal
to the downstream
molecules